AJNR

Predicting Cerebral Ischemic Infarct Volume with Diffusion and Perfusion MR Imaging

Pamela W. Schaefer, George J. Hunter, Julian He, Leena M. Hamberg, A. Gregory Sorensen, Lee H. Schwamm, Walter J. Koroshetz and R. Gilberto Gonzalez

AJNR Am J Neuroradiol 2002, 23 (10) 1785-1794
http://www.ajnr.org/content/23/10/1785

Predicting Cerebral Ischemic Infarct Volume with Diffusion and Perfusion MR Imaging

Pamela W. Schaefer, George J. Hunter, Julian He, Leena M. Hamberg, A. Gregory Sorensen, Lee H. Schwamm, Walter J. Koroshetz, and R. Gilberto Gonzalez

BACKGROUND AND PURPOSE: **Diffusion and perfusion MR imaging have proved useful in the assessment of acute stroke. We evaluated the utility of these techniques in detecting acute ischemic infarction and in predicting final infarct size.**

METHODS: **Diffusion and hemodynamic images were obtained in 134 patients within a mean of 12.3 hours of onset of acute ischemic stroke symptoms. We retrospectively reviewed patient radiology reports to determine the presence or absence of lesion identification on initial diffusion- (DW) and perfusion-weighted (PW) images. Radiologists were not blinded to the initial clinical assessment. For determination of sensitivity and specificity, the final discharge diagnosis was used as the criterion standard. Neurologists were not blinded to the DW or PW imaging findings. In 81 patients, acute lesions were compared with final infarct volumes.**

RESULTS: **Sensitivities of DW imaging and cerebral blood volume (CBV), cerebral blood flow (CBF), and mean transit time (MTT) perfusion parameters were 94%, 74%, 84%, and 84%, respectively. Specificities of DW imaging, CBV, CBF, and MTT were 96%, 100%, 96%, and 96%, respectively. Results were similar in 93 patients imaged within 12 hours. In 81 patients with follow-up, regression analysis yielded $r^2 = 0.9$, slope = 1.24 for DW imaging; $r^2 = 0.84$, slope = 1 .22 for CBV; $r^2 = 0.35$, slope = 0.44 for CBF; and $r^2 = 0.22$, slope = 0.32 for MTT, versus follow-up volume. A DW-CBV mismatch predicted additional lesion growth, whereas DW-CBF and DW-MTT mismatches did not. Results were similar in 60 patients imaged within 12 hours.**

CONCLUSION: **Diffusion and hemodynamic images are sensitive and specific for detecting acute infarction. DW imaging and CBV best predict final infarct volume. DW-CBV mismatch predicts lesion growth into the CBV abnormality. CBF and MTT help identify additional tissue with altered perfusion but have lower correlation with final volume.**

New thrombolytic and neuroprotective therapies are being approved and developed for the treatment of acute ischemic stroke. Although they may salvage tissue characterized by reversible ischemia, these therapies are associated with potential risks, such as development of intracranial hemorrhage. To apply these therapies appropriately, it is important to distinguish between the amount of tissue that is destined to infarct and the tissue that is ischemic but may potentially be salvaged if reperfusion is attempted.

Relatively new MR imaging techniques are improving our ability to evaluate acute stroke. Echo-planar diffusion-weighted (DW) imaging measures the restriction of water movement associated with cytotoxic edema and is sensitive to ischemia within minutes after onset (1–7). Echo-planar perfusion-weighted (PW) imaging can demonstrate the altered physiologic state of the cerebral vasculature immediately after an occlusive or partially occlusive event. This physiologic state may be characterized by parameters of tissue perfusion such as cerebral blood volume (CBV), cerebral blood flow (CBF), and mean transit time (MTT) (8–13). PW imaging allows assessment of alterations in perfusion during acute ischemia (14–24).

DW imaging depicts acute ischemic injury with high sensitivity (86–100%) and specificity (88–100%) at early time points (25–28). Few reports have addressed the sensitivity and specificity of PW imaging in the detection of acute ischemic stroke (14, 16). Furthermore, few reports have compared DW and

Received November 18, 2001; accepted after revision June 21, 2002 .

From the Departments of Radiology (P.W.S., G.J.H., J.H., L.M.H., A.G.S., R.G.G.) and Neurology (L.H.S., W.J.K.), Massachusetts General Hospital, Harvard Medical School, Boston.

Presented in part at the annual meetings of the Radiological Society of North America, Chicago, 2000, and the American Society of Neuroradiology, Boston, 2001.

Address reprint requests to Pamela W. Schaefer, MD, Department of Radiology, Division of Neuroradiology, Gray B285, Massachusetts General Hospital, Fruit Street, Boston, MA 02114; e-mail: pschaefer@partners.org

PW imaging in the detection of acute ischemic injury and in the prediction of final infarct size (14–17, 20–22, 29). These studies are characterized by patient populations of 50 or less and by widely varying results depending on type of perfusion map analyzed, analysis paradigm used, lesion type, time of imaging with respect to ictus, and time of follow-up imaging.

The purposes of this study were 1) to determine the sensitivity and specificity of DW imaging and three perfusion parameters (CBV, CBF, and MTT) in demonstrating ischemic infarction in a large patient population with many different infarction types, and 2) to establish the predictive value of DW imaging, CBV, CBF, and MTT in determining final infarct size in all patients, as well as in those with a perfusion-diffusion mismatch.

Methods

Patient Selection

All patients who presented to the emergency department with signs and symptoms of acute stroke between October 1994 and August 1998 were reviewed. Inclusion criteria for subsequent analysis were considered in two groups. For the evaluation of sensitivities and specificities, all 134 patients with clinical follow-up and who had undergone DW and PW imaging were included in the analysis. For the quantitative prediction of infarction volumes, 81 patients met the inclusion criteria, which were 1) availability of conventional MR, DW, and PW image data sets obtained at the time of presentation to the emergency department; 2) availability of follow-up sectional images with either CT or MR imaging; and 3) demonstration of an infarction on follow-up images. Twenty patients had been included in a previous report (17).

Imaging

MR imaging was performed with a 1.5-T whole-body imager (Signa; GE Medical Systems, Milwaukee, WI) with an echo-planar retrofit (Advanced NMR Systems, Wilmington, MA).

DW images were obtained by using single-shot, echo-planar imaging with sampling of the entire diffusion tensor. Six high–b value images corresponding to diffusion measurements in different gradient directions were acquired, followed by a single low–b value image. The high b value was 1221 mm^2/s, and the low b value was 3 mm^2/s. Imaging parameters were 6000/118 (TR/TE), field of view (FOV) of 40 × 20 cm, image matrix of 256 × 128 pixels, section thickness of 6 mm with a 1-mm gap, 20 axial sections, and three signal averages. Isotropic DW images were generated off-line on a network workstation (Sparcstation 20; Sun Microsystems, Milpitas, CA). Apparent diffusion coefficient (ADC) maps also were generated and used to confirm restricted diffusion. This methodology has been previously described in detail (17, 20).

PW images were acquired with spin-echo (116 patients) or gradient-echo (18 patients) echo-planar techniques during the injection of 0.1 mmol (gradient-echo) or 0.2 mmol (spin-echo) per kilogram of body weight gadodiamide (Omniscan; Nycomed, Oslo, Norway) or gadopentetate dimeglumine (Magnevist; Berlex Laboratories, Wayne, NJ). For the spin-echo echo-planar technique, 51 single-shot echo-planar images were obtained in each of 10 sections, in 83 seconds. Imaging parameters were 1500/75, FOV of 40 × 20 cm, image matrix of 256 × 128 pixels, section thickness of 6 mm with a 1-mm gap. For the gradient-echo echo-planar technique, 46 single-shot echo-planar images were obtained in each of 11 sections, in 69 seconds. Imaging parameters were 1500/50, FOV of 40 × 20 cm, image matrix of 256 × 256 pixels, section thickness of 6 mm with a 1-mm gap. Parametric maps of vascular physiologic function were synthesized by using an arterial input deconvolution paradigm that is described in detail elsewhere (17). In brief, for each voxel, the time-intensity curve observed during the passage of contrast material is converted to a curve of change in 1/T2 (ΔR2), a parameter related to the concentration of gadolinium present in the voxel. An arterial input curve is identified from the ipsilateral middle cerebral artery. Then, for each target voxel, a combination of numerical integration of its ΔR2-time curve and deconvolution between the arterial input and the ΔR2 curve is performed. This yields parameters of CBV, CBF, and MTT. Details of the theory and methodology of the perfusion map calculations have been previously described in detail (9–12, 17)

Fast spin-echo T2-weighted images were acquired with 4200/102 (TR/TE effective), FOV of 20 cm, acquisition matrix of 256 × 256 pixels, section thickness of 5 mm with a 1-mm gap, and one signal average.

CT of the head was performed by using a helical scanner (Advantage; GE Medical Systems, Waukesha, WI), with 5-mm contiguous axial sections with 140 kVp, 340 mAs, and 1-second scanning time.

Image analysis

Patient radiology reports were retrospectively reviewed to determine the presence or absence of lesion identification on the initial DW and PW images. Radiologist interpretations were based on neuroimaging findings and initial clinical assessment, without attempt to blind the radiologists to the neurologists' findings. For determination of sensitivity and specificity, the final discharge diagnosis was used as the criterion standard. The final diagnosis was based on initial and follow-up clinical assessments and neuroimaging studies, without attempt to blind the neurologists to the DW or PW imaging findings.

Visually identified abnormalities on initial DW and PW images, as well as the follow-up images, were outlined by using a commercial image display and analysis program (ALICE; Hayden Image Processing Solutions, Denver, CO). Section by section, lesion contours were generated by using a semiautomated method based on threshold values between normal and abnormal regions and manually corrected by consensus of two radiologists (J.H. and P.W.S.). This was repeated for all volumes in 20 patients so we could measure intraobserver variability. We used this technique rather than a numeric threshold technique because we wanted to simulate how these maps are currently used in clinical practice. Lesion volumes were calculated by summing the individual section lesion areas multiplied by section separation (ie, section thickness plus intersection gap).

Once the volumes were calculated, the data were subdivided into categories based on the differences in apparent lesion volume between DW images and PW parameters. We classified a finding as a mismatch only when the PW image lesion volume was more than 20% larger than the DW image lesion volume. This approach was adopted to minimize errors owing to partial volume effects and head positioning. We used a similar definition of mismatch in a prior report (17)

Statistical Analysis

In all 134 patients, measures of sensitivity, specificity, and predictive values were obtained by using the clinically derived final diagnosis of stroke or no stroke as the criterion standard for ischemic cerebral infarction. These measures were repeated in the 90 patients who were imaged initially within 12 hours.

In all 81 patients with follow-up imaging, statistical analysis of covariance was performed by using a General Linear Model Paradigm (SAS Institute, Cary, NC). The variables tested were final volumes of infarction as predicted by DW imaging and CBV, CBF, and MTT perfusion parameters, arranged into groups based on age, sex, lesion volume mismatch, time of imaging with respect to stroke ictus, and type of infarction.

TABLE: Sensitivity and specificity of DW imaging and perfusion parameters in 134 patients

Technique	Final Diagnosis		Sensitivity (%)	Specificity (%)	PPV (%)	NPV (%)	FP	FN
	Positive	Negative						
DWI								
Positive	101	1	94	96	99	81	1	6
Negative	6	26						
CBV								
Positive	78	0	74	100	100	50	0	28
Negative	28	28						
CBF								
Positive	89	1	84	96	99	59	1	18
Negative	18	26						
MTT								
Positive	89	1	84	96	99	59	1	18
Negative	18	26						

Note.—FN indicates false-negative findings; FP, false-positive findings; NPV, negative predictive value; PPV, positive predictive value.

Subsequently, linear correlations were individually performed for DW imaging, CBV, CBF, and MTT versus follow-up infarct volumes, with the intercept fixed at the origin. In addition, linear correlations were performed for CBV and DW imaging versus follow-up infarct volume in patients with a DW-CBV mismatch. Linear correlations were also performed for CBF and DW imaging versus follow-up infarct volume in patients with a DW-CBF mismatch. Finally, linear correlations were performed for MTT and DW imaging versus follow-up infarct volume in patients with DW-MTT mismatch. Among the 81 patients with follow-up imaging, the linear correlations were repeated in the 60 patients who were imaged initially within 12 hours.

Intraobserver variability was measured by repeating volume measurements in 20 patients. For DW imaging, the initial 20 volume measurements were compared with the second 20 volume measurements with use of a two-tailed *t* test. Subsequently, the difference was obtained for each pair of measurements. The mean and standard deviation of the differences was obtained. This was repeated for CBV, CBF, MTT, and follow-up volumes.

Results

Of 134 patients eligible for entry into the study, all had follow-up clinical evaluation and were grouped on this basis into stroke or non-stroke categories. There were 82 men and 52 women aged 20–93 years (mean age, 65 years). Time from stroke onset to imaging ranged from 43 minutes to 134 hours, with a mean of 12.28 hours. Of the 134 patients, 121 were imaged within 24 hours; 106 patients had a final clinical diagnosis of stroke. On the basis of MR angiography and lesion location on conventional MR images, there were 33 proximal embolic infarctions (four at the top of the internal carotid artery, 24 in the middle cerebral artery, and five in the posterior cerebral artery), 22 lacunar infarctions, 45 distal embolic infarctions, and six watershed infarctions; 28 patients did not have a final clinical diagnosis of stroke. The sensitivity, specificity, and predictive values of DW imaging and CBV, CBF, and MTT perfusion parameters in detecting acute infarction are presented in the Table.

The sensitivities of DW imaging, CBV, CBF, and MTT to be abnormal in the appropriate vascular territory in the setting of a clinical diagnosis of acute stroke were 94%, 74%, 84%, and 84%, respectively. The negative predictive values were 81%, 50%, 59%, and 59%, respectively. On DW images, there were six false-negative findings (ie, patients with clinical stroke but without initial imaging evidence of infarction). These included one acute-on-chronic middle cerebral artery infarction, two pontine lacunar infarctions seen on follow-up DW images, one lateral medullary lacunar infarction that was below the first section on the initial DW images but seen on follow-up DW images, and two presumed lacunar infarctions (one basal ganglia and one pontine) that were not seen on initial or follow-up images, but clinical symptoms persisted in these two patients. False-negative lesions on the CBV images included 16 small distal infarctions, 10 lacunar infarctions, and two watershed infarctions. False-negative lesions on the CBF and MTT images included 10 distal infarctions, six lacunar infarctions, and two watershed infarctions.

The specificities of DW imaging, CBV, CBF and MTT to be abnormal in the appropriate vascular territory in the setting of a clinical diagnosis of acute stroke were 96%, 100%, 96%, and 96%, respectively. The positive predictive values were 99%, 100%, 99%, and 99%, respectively. One false-positive lesion on DW images was a punctate lesion consistent with a distal embolic infarction in a patient in whom the final clinical diagnosis was transient ischemic attack. There was also a DW negative case in which both the CBF and MTT maps demonstrated a hypoperfused area in the left frontal lobe that did not demonstrate tissue injury on follow-up studies.

For the 93 patients imaged within 12 hours, measures of sensitivity, specificity, and predictive values were similar. The sensitivities of DW imaging, CBV, CBF, and MTT to be abnormal in the appropriate vascular territory in the setting of a clinical diagnosis of acute stroke were 92%, 74%, 84%, and 84%, respectively. For each technique, respectively, the negative predictive values were 75%, 49%, 60%, and 60%; specificities, 95%, 95%, 95%, and 95%; and positive predictive values, 99%, 98%, 98%, and 98%.

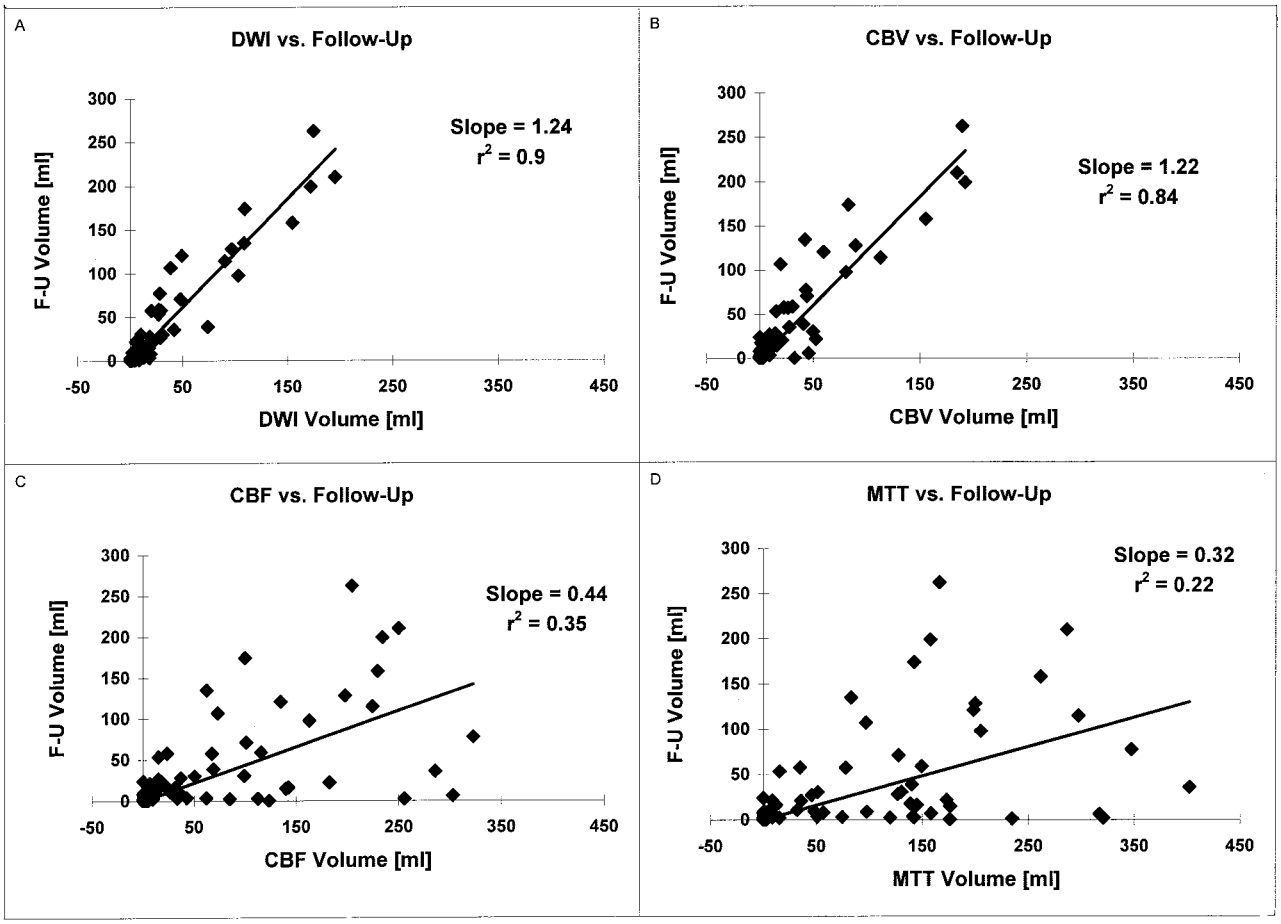

FIG 1. *A–D,* Scatterplots demonstrate initial lesion volume with each technique versus final lesion volume at follow-up (*F-U*) in 81 patients.

A, Initial DW imaging versus follow-up: $r^2 = 0.9$, slope = 1 .24 ± 0.08 (95% confidence limits).
B, Initial CBV versus follow-up: $r^2 = 0.84$, slope = 1 .22 ± 0.11.
C, Initial CBF versus follow-up: $r^2 = 0.35$, slope = 0.44 ± 0.09.
D, Initial MTT versus follow-up: $r^2 = 0.22$, slope = 0.32 ± 0.08.
r^2 indicates coefficient of determination.

Of the 134 patients reviewed, 81 fulfilled the image selection criteria for further analysis. There were 51 men and 30 women aged 21–93 years (mean age, 64.7 years). Time from stroke onset to imaging was 0.72–41.6 hours, with a mean of 7.86 hours; 77 of 81 patients were imaged within 24 hours. Follow-up imaging was available from 1 to 210 days, with a mean of 12.44 days. No patients received intraarterial thrombolytics. One patient received intravenous tissue plasminogen activator, one received intraarterial papaverine, and three received growth factor. All other patients received conventional treatments such as antithrombotic agents, blood pressure titration, and volume expansion, only. There were 25 proximal embolic infarctions (17 in the middle cerebral artery stem, one at the top of the internal carotid artery, two involving both the distal internal carotid artery and proximal middle cerebral artery stem, four in the posterior cerebral artery stem, and one in the superior cerebellar artery stem), 18 lacunar infarctions, and 38 distal infarctions.

Analysis of covariance demonstrated that DW imaging best predicted final infarct volume and that CBV alone of the other perfusion parameters significantly improved the DW imaging prediction of final infarct volume.

Scatterplots of final infarct volumes against initial DW imaging, CBV, CBF, and MTT volumes for all 81 patients are shown in Fig 1. They include the slopes and coefficients of determination (r^2) from regression analyses, with intercept fixed at the origin. The DW images had the highest correlation to a linear fit. Of the perfusion parameters, CBV had the highest correlation to a linear fit.

Scatterplots (not shown) of final infarct volumes against initial DW imaging, CBV, CBF, and MTT volumes for 60 patients imaged within 12 hours demonstrated similar results: for DW imaging versus follow-up infarct volume, $r^2 = 0.91$, slope = 1.21; for CBV versus follow-up, $r^2 = 0.84$, slope = 1.16; for CBF versus follow-up, $r^2 = 0.39$, slope = 0.41; and for MTT, $r^2 = 0.26$, slope = 0.29.

Fig 2 shows scatterplots of final infarct volumes against initial DW imaging, CBV, CBF, and MTT volumes for all patients with follow-up images demonstrating infarction and a perfusion lesion more

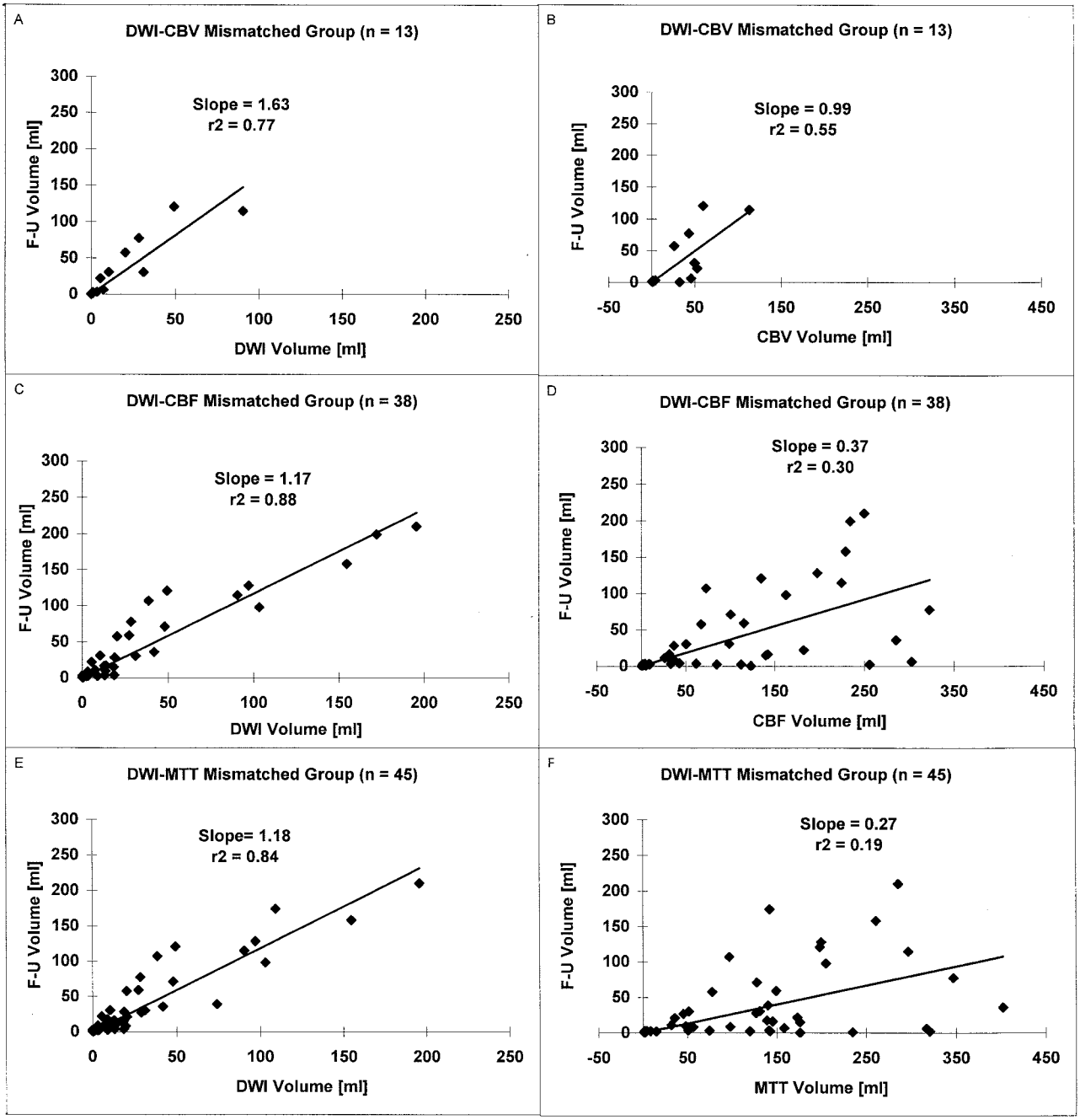

FIG 2. *A–F*, Scatterplots show initial lesion volume versus final infarct volume in patients with a perfusion-diffusion mismatch (perfusion lesion more than 20% larger than the diffusion lesion).

A and *B*, DW-CBV mismatch group: For DW imaging versus follow-up, the regression line was significantly different from the line of identity ($P < .001$). For CBV versus follow-up, the regression line was not significantly different from the line of identity ($P = .18$).

C and *D*, DW-CBF mismatch group: For DW imaging versus follow-up and for CBF versus follow-up, the line of regression was significantly different from the line of identity ($P < .001$).

E and *F*, DW-MTT mismatch group: For DW imaging versus follow-up and for MTT versus follow-up, the line of regression was significantly different from the line of identity ($P < .001$). r^2 indicates coefficient of determination.

than 20% larger than the diffusion lesion (perfusion-diffusion mismatch). All patients with a DW-CBV mismatch also had a DW-MTT mismatch.

Scatterplots (not shown) of final infarct volumes against initial DW imaging, CBV, CBF, and MTT volumes for the patients with a diffusion-perfusion mismatch who were imaged within 12 hours demonstrated similar results. There were 11 patients in the DW-CBV mismatch group: for regression of DW imaging against follow-up volume, slope = 1.43, r^2 = 0.77; for CBV against follow-up volume, slope = 1.02, r^2 = 0.49. There were 30 patients in the DW-CBF mismatch group: for regression of DW imaging against follow-up volume, slope = 1.08, r^2 = 0.90; for CBF against follow-up volume, slope = 0.36, r^2 = 0.34. There were 34 patients in the DW-MTT mis-

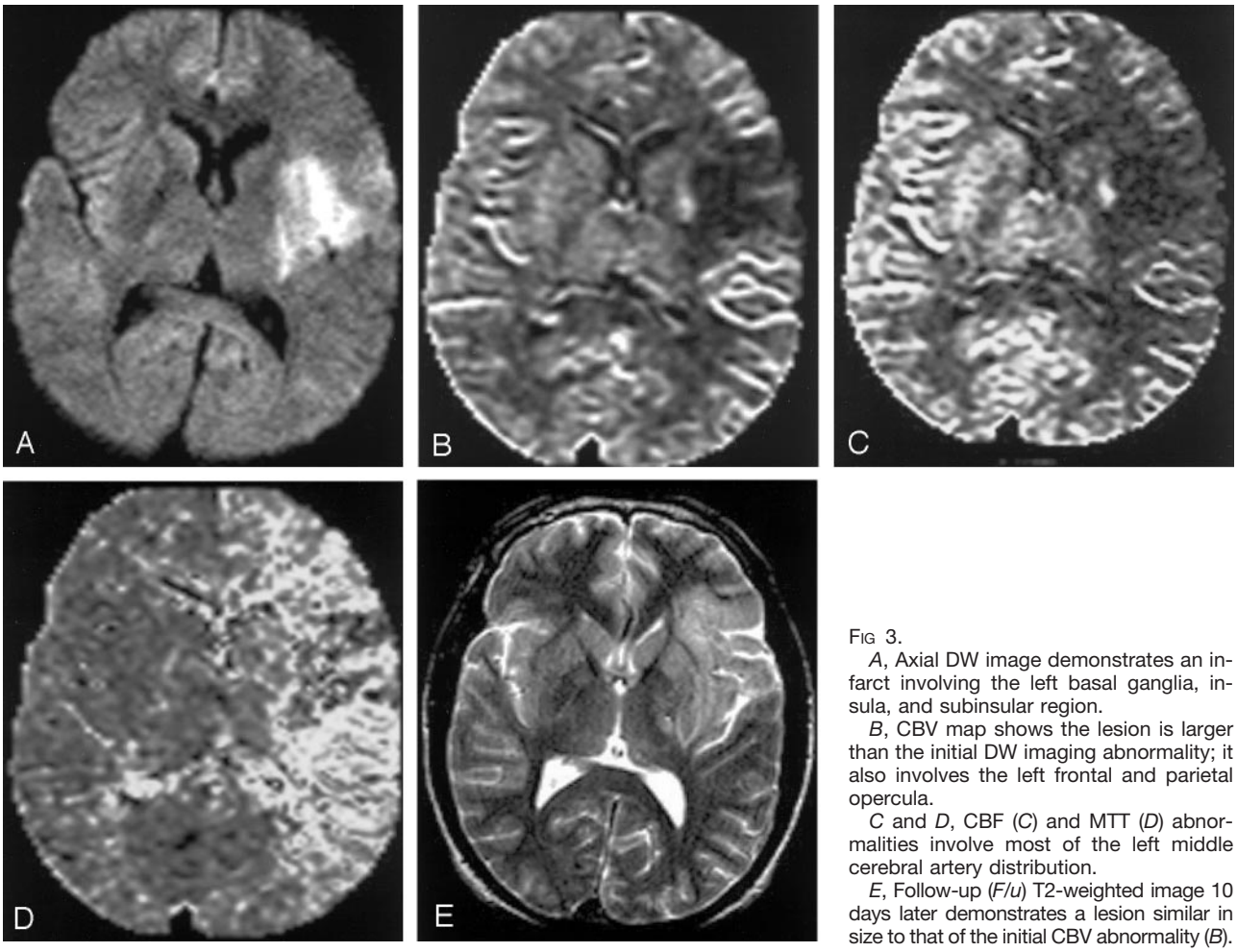

FIG 3.
A, Axial DW image demonstrates an infarct involving the left basal ganglia, insula, and subinsular region.
B, CBV map shows the lesion is larger than the initial DW imaging abnormality; it also involves the left frontal and parietal opercula.
C and *D*, CBF (*C*) and MTT (*D*) abnormalities involve most of the left middle cerebral artery distribution.
E, Follow-up (*F/u*) T2-weighted image 10 days later demonstrates a lesion similar in size to that of the initial CBV abnormality (*B*).

match group: for regression of DW imaging against follow-up volume, slope = 1.10, $r^2 = 0.84$; for MTT against follow-up volume, slope = 0.24, $r^2 = 0.19$.

Intraobserver variability analysis in 20 cases revealed the following: for DW imaging, initial mean volume = 44.829 cm^3, second mean volume = 44.558 cm^3, mean (± SD) difference = 0.271 ± 0.672 cm^3; for CBV, initial mean volume = 45.029 cm^3, second mean volume = 45.433 cm^3, mean difference = – 0.405 ± 5.310 cm^3; for CBF, initial mean volume = 132.659 cm^3, second mean volume = 127.996 cm^3, mean difference = 4.663 ± 13.178 cm^3; for MTT, initial mean volume = 161.556 cm^3, second mean volume = 159.131 cm^3, and mean difference = 2.425 ± 5.744 cm^3; and for final infarct volume, initial mean volume = 61.120 cm^3, second mean volume = 60.386 cm^3, mean difference = 0.734 ± 1.977 cm^3. The initial 20 volume measurements were not significantly different from the second 20 volume measurements ($P > .05$) for DW imaging, CBV, CBF, MTT, or final infarct volume.

Fig 3 demonstrates images of a patient with a proximal left middle cerebral artery embolus. The CBV, CBF, and MTT lesion volumes were more than 20% larger than the DW imaging lesion volume. As predicted from our data, the final infarct volume was larger than the initial DW imaging lesion volume, similar to the initial CBV lesion volume and much smaller than the initial CBF or MTT lesion volumes.

Fig 4 compares the percentage of diffusion-perfusion mismatches in proximal embolic versus nonproximal (distal or lacunar) infarctions in the 81 patients with follow-up imaging. There were 25 proximal occlusions (17 middle cerebral artery stem, one internal carotid artery, two internal carotid artery and middle cerebral artery stem, four posterior cerebral artery stem, and one superior cerebellar artery stem) and 56 nonproximal occlusions (18 lacunar and 38 distal embolic). For proximal occlusions, 28% of patients had a DW-CBV mismatch; 72%, a DW-CBF mismatch; and 80%, a DW-MTT mismatch. For distal occlusions, 11% of patients had a DW-CBV mismatch; 38%, a DW-CBF mismatch; and 41%, a DW-MTT mismatch.

Discussion

Our results demonstrate that early DW imaging is highly effective in detecting acute ischemic infarction and in predicting final ischemic cerebral infarct volume. In specific circumstances, PW imaging provides additional predictive power. Of the calculated MR hemodynamic parameters, CBV maps appeared su-

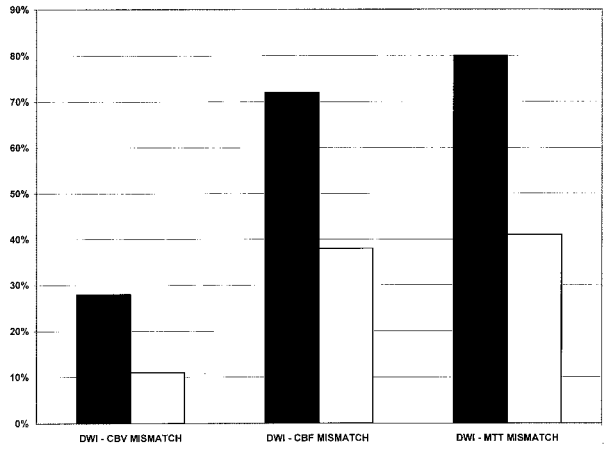

FIG 4. Percentage of patients with diffusion-perfusion mismatches for proximal (black bars) and nonproximal (white bars) infarctions.

perior to CBF and MTT maps in predicting final infarct volume. CBV maps are most informative in cases of a DW-CBV mismatch, which most commonly occur with proximal cerebral arterial occlusions.

DW imaging was highly sensitive (94%) and specific (96%) in the large patient population that we studied. These values are consistent with reported sensitivities of 88–100% and reported specificities of 86–100% (25–28). In our patient population, lesions missed on DW images generally fell into two categories: 1) deep gray nuclei and brain-stem lacunes that are seen as punctate lesions on follow-up images or are presumed on the basis of persistent clinical deficits, and 2) ischemic but viable lesions, with hypoperfusion and normal DW images and ADC maps, that progress to infarction. These observations are similar to those of Ay et al (30). False-positive lesions are rare. A false-positive lesion on DW images occurred in one patient who had a transient ischemic attack with a tiny lesion that was hyperintense on DW and T2-weighted images, consistent with a tiny distal embolus that was clinically silent. Nearly 50% of patients with transient ischemic attacks are known to have small hyperintense lesions on DW images in the appropriate vascular territory (31). False-positive lesions have been reported with cerebral abscess (with restricted diffusion on the basis of viscosity) and tumor (with restricted diffusion on the basis of attenuated cell packing) (26). When these lesions are viewed in combination with other routine T1- and T2-weighted MR images, they should be easily differentiated from acute infarctions. A false-positive lesion also was reported in a patient with a subacute infarction; the lesion proved to be hyperintense on DW images secondary to an increase in the T2 signal intensity (25). This "T2 shine through" effect can easily be resolved by interpreting the DW images in combination with ADC maps, which do not have a T2 component. Acute ischemic lesions with restricted diffusion are hypointense on ADC maps.

We found that, in general, PW images are less sensitive than DW images in the detection of acute stroke. Lesions missed on PW images included lesions with small abnormalities on DW images that were not detected because of the lower resolution of PW images, and lesions with early reperfusion. Our results agree with those of Ueda et al (16) that CBF and MTT maps are more sensitive than CBV maps but less specific.

The role of PW imaging in conjunction with DW imaging is being elucidated. The most important clinical effect may result from defining an ischemic penumbra, a region that is ischemic but still viable and may progress to infarction. Consequently, investigation has focused on strokes with a diffusion-perfusion mismatch. One clear observation is that proximal occlusions are far more likely to result in a diffusion-perfusion mismatch than are distal or lacunar infarctions. Operationally, in the absence of thrombolysis, the diffusion abnormality is thought to represent the ischemic core and the region characterized by normal diffusion, but abnormal perfusion may represent the ischemic penumbra. Definition of the penumbra is complicated because there are multiple hemodynamic parameters that may be calculated from the perfusion MR imaging data. Previously, it has not been clear which hemodynamic maps (eg, CBF, CBV, and MTT) are most informative in predicting final infarct volume. The data presented are in agreement with previously published reports (14–17, 19, 21, 22, 29) and provide insights into this issue (Fig 2).

In all patients in this study, of all parameters measured (DW imaging, CBV, CBF and MTT), DW imaging correlated most highly with final infarct volume, with an r^2 of 0.90 in all patients and 0.91 in those patients imaged within 12 hours. This is within the range of previously reported values of 0.69–0.98 (15, 17, 19, 22). Predicted lesion growth was 24% in all patients and 21% in those patients imaged within 12 hours. Reported lesion growth ranges from 32% to 144% (14, 15, 17, 19, 21, 22). This variability likely results from variability in timing of reperfusion, blood pressure, collateral perfusion and postischemic tissue responses, as well as initial and follow-up imaging times. Some patients in the literature were imaged at even earlier time points when less initial lesion growth would have occurred. Also, our mean follow-up time of 12 days was later than that of some other studies. At 12 days, resolution of edema but not tissue atrophy would have occurred.

Of the perfusion parameters, overall, CBV correlated best with final infarct volume and had a very high correlation, with an r^2 of 0.84, in all patients as well as in those imaged within 12 hours. This is similar to previously reported values ranging from 0.79 to 0.81 (17, 29). Predicted lesion growth from the initial CBV abnormality to the final infarct size was 22% in all patients and 16% in those patients imaged within 12 hours. This is similar to the 27% predicted lesion growth reported by Sorensen et al (17) in a smaller series. In the study by Ueda et al (16), lesions decreased in size from the initial CBV abnormality. Their follow-up images were obtained at 8.9 months, a time point at which atrophy of the infarcted tissue

would have occurred. Overall, CBF and MTT demonstrated very poor correlations with final infarct volume (r^2 of 0.35 in all patients and 0.39 in patients imaged in less than 12 hours for CBF and r^2 of 0.22 in all patients and 0.26 in patients imaged in less than 12 hours for MTT). These findings are similar to reported values of r^2 of 0.3–0.67 for CBF and r^2 of 0.3–0.69 for MTT (14, 17, 21, 29). Furthermore both CBF and MTT greatly overestimated final infarct size. Predicted final infarct size was 44% for all patients and 41% for patients imaged within 12 hours of the initial CBF abnormality, and 32% for all patients and 29% for patients imaged within 12 hours of the initial MTT abnormality.

When there is a DW-CBV, DW-CBF, or DW-MTT mismatch, DW imaging continued to correlate highly with final infarct volume (r^2 of 0.77, 0.88, 0.84, respectively, for all patients and r^2 of 0.77, 0.90, 0.85 for patients imaged within 12 hours) and correlated better with final infarct volume than did the respective perfusion parameter. Of the perfusion parameters, in these patients, CBV appeared superior to CBF and MTT in predicting final infarct volume. A DW-CBV mismatch was found in 16% of all patients studied and in 18% of those patients who presented within 12 hours. The correlation of the CBV abnormality with the final infarct was statistically significant, with a slope of 0.99 and r^2 of 0.55 for all patients and a slope of 1.02 and r^2 of 0.49 for patients imaged within 12 hours. The predicted lesion growth from DW imaging to final infarct was 63% in all patients and 43% in patients imaged within 12 hours. These data indicate that when a DW-CBV mismatch exists, infarcts grow to the size of the CBV abnormality. Thus, patients with a DW-CBV mismatch are predicted to have the most lesion growth and may benefit most from any perfusion-altering therapies such as hypertension, thrombolysis, neuroprotective agents, angioplasty, and hypothermia.

While diffusion-perfusion mismatches were more commonly observed with CBF and MTT maps, the predictive power of these maps was poor and inferior to the predictive power of CBV maps. In fact, with a mismatch defined as a perfusion lesion more than 20% larger than the diffusion lesion, in patients with a DW-CBF or DW-MTT mismatch, predicted lesion growth from DW imaging to final infarct remained at approximately 20%. It was not larger than predicted growth in all patients. Thus, it appears that at the time points addressed in this study, CBF and MTT are sensitive to hemodynamic changes, but such changes may not be injurious. Further quantification of CBF and MTT may improve their ability to discriminate between critically ischemic regions and regions of minor hemodynamic change.

The PW imaging observations are best interpreted with reference to positron emission tomography (PET) hemodynamic stroke studies (32). These studies have demonstrated that in the early stages of ischemia, decreased cerebral perfusion pressure produces vasodilatation and an increase in CBV, which maintains constant CBF and oxygen extraction fraction. With further reduction of cerebral perfusion pressure, the compensatory vasodilatation reaches a maximum. After this, the CBF begins to fall, but there is compensatory increase in the oxygen extraction fraction. With continued decreases in cerebral perfusion pressure and CBF, the CBV begins to decrease due to collapse of capillary beds, and the oxygen extraction fraction reaches its maximum. Once the oxygen extraction is maximal, further declines in CBF and CBV result in disruption of cellular function, and clinical symptoms develop.

Considering the findings from PET, we speculate that the high correlation between CBV and final infarct volume is best explained in the following manner. When the CBV is abnormal, the CBF is usually below the threshold for tissue viability and there is usually an associated DW imaging abnormality. In fact, we observed no cases in which there was a CBV abnormality but normal DW images. Likewise, except for small lesions below the resolution of CBV maps, we did not observe abnormal DW images but normal CBV. When there is a DW-CBV mismatch, the CBF in the mismatched region is likely close to the threshold for tissue viability and the infarct usually grows into this CBV area at risk. Likewise, these physiologic changes suggest why CBF and MTT are more sensitive than CBV, less specific than CBV, and poor indicators of final infarct size. In the setting of normal or elevated CBV, MTT and CBF may be abnormal but CBF is well above the threshold for tissue infarction. The tissue may progress to infarction, but if collateralization is present and/or early reperfusion occurs, then the blood flow may be restored and there may be no permanent tissue damage. This could also explain why DW- CBF and DW-MTT mismatches are more common than DW-CBV mismatches.

Despite significant correlations between DW and PW imaging, precise prediction of final infarct volume in individual cases remains elusive. This is because stroke is very heterogeneous and multifactorial. Stroke evolution depends on factors such as duration of ischemia, degree of ischemia, presence of prior ischemia, timing of spontaneous recanalization, distal migration of emboli, integrity of the circle of Willis and leptomeningeal collateral vessels, and systemic hemodynamic factors. Our data demonstrate that infarct growth sometimes does not occur in the setting of a DW-CBV mismatch and sometimes does occur despite the absence of a mismatch. Furthermore, whereas the DW imaging abnormality is thought to represent the ischemic core, a number of animal studies have demonstrated abnormal regions on DW images that did not progress to infarction (33–36). In addition, rare cases of reversibility on DW images have been reported in humans who received conventional stroke therapy (37). Furthermore, humans treated with intravenous or intraarterial tissue plasminogen activator may have regions of reversibility on DW images (38). Also, Ueda et al (16) reported four patients with ADC hypointensity with restricted diffusion who did not have infarctions on follow-up images.

The limitations of our study relate to the observational study design. Routine clinical management including decisions on timing of imaging studies was not altered for the purposes of this investigation. Thus, time of initial and follow-up imaging was variable, and follow-up imaging was with CT or MR imaging. Futhermore, in this study, we did not address the role of DW and PW imaging in patient triage, treatment, or management nor did we address the influence of these factors on lesion growth. Nevertheless, our conclusions with respect to the principal findings should be robust because all patients underwent initial imaging by means of the four methods (DW imaging, CBV, CBF, and MTT) that we evaluated. It is unlikely that the design would bias one method over the other.

Conclusion

In a large patient population with a wide variety of infarction types, we have demonstrated that DW imaging is highly sensitive in the detection of acute ischemic stroke and is more sensitive than CBV, CBF, or MTT images. DW imaging findings correlate highly with final infarct volume even if there is a DW-CBV, DW-CBF, or DW-MTT mismatch. CBV also correlates highly with final infarct volume. When there is a DW-CBV mismatch, predicted lesion growth is 63% and to the size of the CBV abnormality. In all other patients, even those with a DW-CBF or DW-MTT mismatch, predicted lesion growth is approximately 20%. While CBF and MTT maps identify altered hemodynamics, predicted lesion growth in patients with a DW-CBF or DW-MTT mismatch is not statistically significantly larger than that in all patients.

Acknowledgments

The authors would like to acknowledge Elkan Halpern, PhD, for his assistance with statistical analysis and Cara O'Reilly for her assistance in manuscript preparation.

References

1. Kucharczyk J, Vexler ZS, Roberts TP, et al. **Echo-planar perfusion-sensitive MR imaging of acute cerebral ischemia**. *Radiology* 1993; 188:711–717
2. Kucharczyk J, Mintorovich J, Asgari H, Moseley M. **Diffusion/perfusion MR imaging of acute cerebral ischemia**. *Magn Reson Med* 1991;19:311–315
3. Moseley M, Kucharczyk J, Mintorovich J, et al. **Diffusion-weighted MR imaging of acute stroke: correlation with T2-weighted and magnetic susceptibility-enhanced MR imaging in cats**. *AJNR Am J Neuroradiol* 1990;11:423–429
4. Moseley M, Cohen Y, Mintorovich J, et al. **Early detection of regional cerebral ischemia in cats: comparison of diffusion- and T2-weighted MRI and spectroscopy**. *Magn Reson Med* 1990;14:330–346
5. Mintorovich J, Moseley M, Chileuitt L, Shimizu H, Cohen Y, Weinstein P. **Comparison of diffusion- and T2-weighted MRI for the early detection of cerebral ischemia and reperfusion in rats**. *Magn Reson Med* 1991;18:39–50
6. Moonen CT, Pekar J, de Vleeschouwer MH, van Gelderen P, van Zijl PC, DesPres D. **Restricted and anisotropic displacement of water in healthy cat brain and in stroke studied by NMR diffusion imaging**. *Magn Reson Med* 1991;19:327–332
7. Matsumoto K, Lo EH, Pierce AR, Garrido L, Kowall NW. **Role of vasogenic edema and tissue cavitation in ischemic evolution on diffusion-weighted imaging: comparison with multiparameter MR and immunohistochemistry**. *AJNR Am J Neuroradiol* 1995;16:1107–1115
8. Belliveau J, Rosen B, Kantor H. **Functional cerebral imaging by susceptibility contrast NMR**. *Magn Reson Med* 1990;14:538–546
9. Ostergaard L, Sorensen AG, Kwong KK, Weisskoff RM, Gyldensted C, Rosen BR. **High-resolution measurement of cerebral blood flow using intravascular tracer bolus passages, II: experimental comparison and preliminary results**. *Magn Reson Med* 1996;36: 726–736
10. Ostergaard L, Weisskoff RM, Chesler DA, Gyldensted C, Rosen BR. **High-resolution measurement of cerebral blood flow using intravascular tracer bolus passages, I: mathematical approach and statistical analysis**. *Magn Reson Med* 1996;36:715–725
11. Rosen BR, Belliveau JW, Vevea JM, Brady TJ. **Perfusion imaging with NMR contrast agents**. *Magn Reson Med* 1990;14:249–265
12. Rosen BR, Belliveau JW, Aronen HJ, et al. **Susceptibility contrast imaging of cerebral blood volume: human experience**. *Magn Reson Med* 1991;22:293–299
13. Rosen BR, Belliveau JW, Buchbinder BR, et al. **Contrast agents and cerebral hemodynamics [review]**. *Magn Reson Med* 1991;19: 285–292
14. Barber P, Darby D, Desmond P, et al. **Prediction of stroke outcome with echo-planar perfusion- and diffusion-weighted MRI**. *Neurology* 1998;51:418–456
15. Tong D, Yenari M, Albers G, O'Brien M, Marks M, Moseley M. **Correlation of perfusion- and diffusion-weighted MRI with NIHSS score in acute (<6.5 hour) ischemic stroke**. *Neurology* 1998;50:864–870
16. Ueda T, Yuh T, Maley J, Quets J, Hahn P, Magnotta V. **Outcome of acute ischemic lesion evaluated by diffusion and perfusion MR imaging**. *AJNR Am J Neuroradiol* 1999;20:983–989
17. Sorensen A, Copen W, Ostergaard L, et al. **Hyperacute stroke: simultaneous measurement of relative cerebral blood volume, relative cerebral blood flow, and mean tissue transit time**. *Radiology* 1999;210:519–527
18. Schwamm L, Koroshetz W, Sorensen A, et al. **Time course of lesion development in patients with acute stroke: serial diffusion and hemodynamic weighted magnetic resonance imaging**. *Stroke* 1998; 29:2268–2276
19. Rordoff G, Koroshetz W, Copen W, et al. **Regional ischemia and ischemic injury in patients with acute middle cerebral artery stroke as defined by early diffusion-weighted and perfusion-weighted MRI**. *Stroke* 1998;29:939–943
20. Sorensen AG, Buonanno FS, Gonzalez RG, et al. **Hyperacute stroke: evaluation with combined multisection diffusion-weighted and hemodynamically weighted echo-planar MR imaging**. *Radiology* 1996;199:391–401
21. Karonen J, Vanninen R, Liu Y, et al. **Combined diffusion and perfusion MRI with correlation to single-photon emission CT in acute ischemic stroke: ischemic penumbra predicts infarct growth**. *Stroke* 1999;30:1583–1590
22. Beaulieu C, de Crespigny A, Tong D, Moseley M, Albers G, Marks M. **Longitudinal magnetic resonance imaging study of diffusion and perfusion in stroke: evolution of lesion volume and correlation with clinical outcome**. *Ann Neurol* 1999;46:568–578
23. Hamberg LM, Macfarlane R, Tasdemiroglu E, et al. **Measurement of cerebrovascular changes in cats after transient ischemia using dynamic magnetic resonance imaging**. *Stroke* 1993;24:444–450
24. Hamberg L, Boccalini P, Stranjalis G, et al. **Continuous assessment of cerebral blood volume in transient ischemia using steady state susceptibility contrast MRI**. *Magn Reson Med* 1996;35:168–173
25. Gonzalez RG, Schaefer PW, Buonanno FS, et al. **Diffusion-weighted MR imaging: diagnostic accuracy in patients imaged within 6 hours of stroke symptom onset**. *Radiology* 1999;210:155–162
26. Lovblad K, Laubach H, Baird A, et al. **Clinical experience with diffusion-weighted MR in patients with acute stroke**. *AJNR Am J Neuroradiol* 1998;19:1061–1066
27. Marks MP, de Crespigny A, Lentz D, Enzmann DR, Albers GW, Moseley ME. **Acute and chronic stroke: navigated spin-echo diffusion-weighted MR imaging**. *Radiology* 1996;199:403–408
28. Singer M, Chong J, Lu D, Schonewille W, Tuhrim S, Atlas S. **Diffusion-weighted MRI in acute subcortical infarction**. *Stroke* 1998;29:133–136
29. Karonen J, Liu Y, Vanninen R, et al. **Combined perfusion and diffusion weighted MR imaging in acute ischemic stroke during the first week: a longitudinal study**. *Radiology* 2000;217:668–694

30. Ay H, Koroshetz W, Buonanno F, et al. **Normal diffusion-weighted MR imaging during stroke-like deficits**. *Neurology* 1999;52:1784–1792
31. Kidwell C, Alger J, DiSalle F, et al. **Diffusion MRI in patients with transient ischemic attacks.** *Stroke* 1999;30:1174–1180
32. Powers W. **Cerebral hemodynamics in ischemic cerebrovascular disease**. Ann Neurol 1991;29:231–240
33. Hasegawa Y, Fisher M, Latour L, Dardzinski B, Sotak C. **MRI diffusion mapping of reversible and irreversible ischemic injury in focal brain ischemia**. *Neurology* 1994;44:1484–1490
34. Muller TB, Haraldseth O, Jones RA, et al. **Combined perfusion- and diffusion-weighted magnetic resonance imaging in a rat model of reversible middle cerebral artery occlusion**. *Stroke* 1995;26:451–457
35. Minematsu K, Li L, Sotak C, Davis M, Fisher M. **Reversible focal ischemic injury demonstrated by diffusion-weighted magnetic resonance imaging**. *Stroke* 1992;23:1304–1310
36. Dardzinski B, Sotak C, Fisher M, Hasegawa Y, Li L, Minematsu K. **Apparent diffusion coefficient mapping of experimental focal cerebral ischemia using diffusion-weighted echo-planar imaging**. *Magn Reson Med* 1993;30:318–325
37. Grant PE, He J, Halpern EF, et al. **Frequency and clinical context of decreased apparent diffusion coefficient reversal in the human brain.** *Radiology* 2001;221:43–50
38. Kidwell C, Saver J, Mattiello J, et al. **Thrombolytic reversal of acute human cerebral ischemic injury shown by diffusion/perfusion magnetic resonance imaging**. *Ann Neurol* 2000;47:462–469